# Heat transport enhanced by optical phonons in one-dimensional anharmonic lattices with alternating bonds

Daxing Xiong,[1,*] Yong Zhang,[2,*] and Hong Zhao[2]
[1]*Department of Physics, Fuzhou University, Fuzhou 350002, Fujian, China*
[2]*Department of Physics and Institute of Theoretical Physics and Astrophysics, Xiamen University, Xiamen 361005, Fujian, China*
(Received 20 June 2013; published 20 November 2013)

In lattice systems, the effects of optical phonons on heat transport are usually neglected due to their relatively small group velocities compared with acoustic phonons, or even assumed to be negative because introducing optical phonons may simultaneously reduce the group velocities of acoustic phonons. In order to well understand the role played by optical phonons, we propose a one-dimensional anharmonic lattice model with alternating interactions, where the optical phonons can be conveniently tuned. We find that in contrast to previous studies, the optical phonons (in coordination with the nonlinearities) can enhance heat transport in the thermodynamical limit, suggesting that optical phonons can also play an active role. The underlying mechanism is related to the effects of two kinds of nonlinear excitations, i.e., the optical and the gap discrete breathers (DBs). These DBs release energy and in turn facilitate heat transport.

DOI: 10.1103/PhysRevE.88.052128 PACS number(s): 44.10.+i, 63.20.−e, 05.60.−k, 64.70.qd

## I. INTRODUCTION

In solid-state physics, the optical phonons are usually believed not to contribute to thermal conduction for their relatively small group velocities compared with acoustic phonons [1]. For this reason the effects of optical phonons are often neglected [2] or even suggested to be negative [3]. However, it should be noted that such a belief is based on the analysis to linear lattices with (approximated) harmonic interactions; anharmonic (or nonlinear) interactions may result in qualitatively different properties. For example, a cubic anharmonicity can cause an optical phonon to split into two acoustic phonons [4] and thereby contribute to heat transport. In fact, recently many exceptions to the mentioned belief have been found in both experimental and numerical studies [5–11]; e.g., Mittal and Mazumder [8] have showed that optical phonons contribute significantly to thermal transport in thin silicon films. Shiomi and Maruyama [9] have performed molecular dynamics simulations of carbon nanotubes; they found the great contribution of optical phonons to the observed non-Fourier heat conduction. But unfortunately, in anharmonic lattices, the mechanism of the interactions between optical phonons and heat transport is still unclear.

To investigate this problem theoretically, such an anharmonic lattice model is necessary: its spectra contains the optical mode on one hand, and its heat transport properties should be easy to investigate on the other hand. A natural candidate satisfying the first requirement is the one-dimensional (1D) diatomic lattice with the Fermi-Pasta-Ulam-$\beta$ (FPU-$\beta$) interparticle interaction, where the mass ratio of the light particles to the heavy particles, denoted by $r$, can be used as a control parameter. However, the heat conduction properties of the diatomic FPU-$\beta$ lattice is hard to access numerically. In this respect, Dhar and Saito [12,13] have performed simulations for some $r$ values. Their results suggest that the heat conductivity $\kappa$ may diverge with the system size $L$ as $\kappa \sim L^{\alpha}$ (where $\alpha$ is a constant), which is in agreement with the generally believed divergence in 1D momentum conserving lattices with symmetric interactions [13–19]. (For 1D momentum conserving lattices with asymmetric interactions, refer to recent progress in Ref. [20].) They have also argued that the divergent exponent $\alpha$ is independent on the mass ratio $r$ and showed that it is about $1/3$, the same as that in monatomic FPU-$\beta$ lattices [12,13]. This argument implies that introducing the optical phonons does not change the value of $\alpha$ and thus does not change the heat transport properties significantly. However, it is worth noting that in their studies, all the reported results of $\kappa$ are for $r$ values that are very close to 1. For small $r$ values, they pointed out that the temperature profile is ill-behaved, implying that there is a serious thermalization problem in this system. Recently, an effort [21] to understand this thermalization problem was made in diatomic harmonic lattices by noting that in any given normal mode, the mean kinetic energy of a particle depends on its mass. In this study, certain stochasticity is added to the dynamics, and it is found that the thermalization problem would be cured in the thermodynamic limit. Obviously, this cannot be the case in FPU-$\beta$ lattices where the dynamics is completely deterministic.

Therefore, the diatomic lattice is not an ideal model to investigate the role the optical phonons may play in heat transport because of the thermalization problem. In order to overcome this difficulty, in this paper we propose a variant lattice, i.e., the lattice with alternating interactions instead. This system not only has tunable phonons, but, as we will show in the following, also is free of the thermalization problem. These advantages are very favorable to our aim here.

In addition to these advantages, we also note that the lattice model with alternating interactions has a linear phonon spectrum, which is very similar to that in diatomic lattices [shown in Sec. II and Fig. 1(b)]. Such a similarity may lead us to expect that both of them would follow a similar heat conduction behavior as well. Therefore, studying the heat conduction properties in one of the systems can provide insights into that in another system. Indeed, the investigations of localization

*Corresponding authors: phyxiongdx@fzu.edu.cn; yzhang75@xmu.edu.cn

 

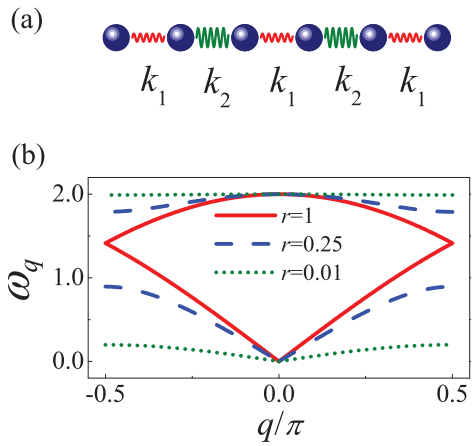


FIG. 1. (Color online) (a) The 1D lattice model with alternating interactions. The interaction strength is denoted as $k_1$ and $k_2$ with $k_1 \leqslant k_2$; (b) the linear phonon dispersion relation of this model for several $r$ ($r = k_1/k_2$).

modes in lattices with graded mass and graded interaction have obtained the equivalent results, which then supports our noting here [22]. Besides, we would like to mention that the alternating lattice is also associated with some real systems, such as the hydrogen-bonded chains with alternating intra- and intermolecular covalent bonding interactions [23], the alternating bond Ising chains (having a nonuniversal critical dynamics by introducing the bonds alternating) [24], and the supperlattices (can be viewed as chains with regularly varying exchange interactions) [25]. In particular, it can model the carbon nanotubes with bond length alternation, since the bond force constant depends on the length. Recently, the thermal conductivity in nanotubes with bond length alternation has been investigated by molecular dynamics and crystal orbital analysis [26]. It has been found that the bond alternation can strongly modify the thermal conductivity in the armchair nanotubes.

With this proposed lattice, we shall carefully examine the heat conduction properties, with the aim to present a strong understanding of the role played by optical phonons. The rest of this article is organized as follows: In Sec. II we shall describe the model, provide its phonon spectra, and analyze why it can avoid the thermalization problem. Section III will present the results of heat conduction. We shall show the divergence of the heat conductivity with the system size and how the heat conductivity is enhanced by introducing optical phonons. Section IV is focused on the underlying mechanism for the enhancement. We shall relate it to the properties of discrete breathers. Finally, our conclusions will be summarized in Sec. V.

## II. MODELS

We consider the 1D lattice model shown schematically in Fig. 1(a). Compared with the diatomic lattice with alternating mass, the model alternates the interactions with coupling strengths $k_1$ and $k_2$ instead. We assume $k_1 \leqslant k_2$ here. The Hamiltonian of this lattice with $L$ ($L$ being even) particles can be represented by

$$H = \sum_{j=1}^{L/2} \left[ \frac{p_{2j-1}^2}{2\mu} + \frac{p_{2j}^2}{2\mu} + k_1 V(x_{2j} - x_{2j-1}) + k_2 V(x_{2j+1} - x_{2j}) \right], \quad (1)$$

where $x_j$ is the displacement of the $j$th particle from its equilibrium position and $p_j$ its momentum. The mass $\mu$ is set to be unit. The interparticle interaction that we mainly focus on is of the FPU-$\beta$ type; i.e., $V(x) = \frac{1}{2}x^2 + \frac{1}{4}x^4$. For demonstrating that the thermalization problem is ubiquitous for diatomic lattices regardless of the types of interactions, the Toda potential [$V(x) = \exp(-x) + x - 1$] is also considered for comparison. Similar to the mass ratio of the diatomic lattice, a crucial control parameter of this lattice is the coupling ratio $r$, which specifies the comparative strength of two adjacent couplings. We denote it as $r = k_1/k_2$ and assume $k_1 + k_2 = 2$, then $r = 1$ corresponds to the monatomic lattice.

To show why such a lattice model is considered, let us see its linear phonon spectra first. Making the harmonic approximation of the interactions in Eq. (1) and according to the Newton's law we have $\ddot{x}_{2j-1} = k_1(x_{2j} - x_{2j-1}) - k_2(x_{2j-1} - x_{2j-2})$ and $\ddot{x}_{2j} = k_2(x_{2j+1} - x_{2j}) - k_1(x_{2j} - x_{2j-1})$. To solve these equations, usually the normal mode solutions (both particles vibrate with the same frequency) of the form $x_{2j-1} = Ae^{[i\omega_q t - iq(2j-1)]}$ and $x_{2j} = Be^{[i\omega_q t - iq(2j)]}$ are supposed, where $q$ is the wave number and $\omega_q$ is the corresponding frequency. Combining the above equations, we get

$$\left(k_1 + k_2 - \omega_q^2\right)A - [k_2 e^{-iq} + k_1 e^{iq}]B = 0; \quad (2)$$

and

$$-[k_1 e^{-iq} + k_2 e^{iq}]A + \left(k_1 + k_2 - \omega_q^2\right)B = 0. \quad (3)$$

Equations (2) and (3) have nontrivial solutions only if the determinant of the coefficient matrix is zero. This yields two roots,

$$\omega_q^{\pm} = \left[k_1 + k_2 \pm \left(k_1^2 + k_2^2 + 2k_1 k_2 \cos 2q\right)^{\frac{1}{2}}\right]^{\frac{1}{2}}, \quad (4)$$

which determines the linear phonon spectra of this lattice. Combining $k_1 + k_2 = 2$, we are then able to plot the phonon spectra for a fixed $r$. The results of the phonon spectrum for several $r$ values are summarized in Fig. 1(b), from which a phonon spectra similar to the diatomic lattice can be clearly seen, i.e., for a given $r$ ($r \neq 1$), the spectra contains an acoustic branch ($\omega_q^-$) and an optical branch ($\omega_q^+$) with a gap bridging them; the width of the gap is determined by $r$, a larger $r$ indicates a wider gap and leads to a smaller group velocity of the acoustic branch.

Next, let us discuss why the thermalization problem is avoided in this lattice. For this purpose we first show the temperature profiles for both lattice models with alternating masses (the diatomic lattices) and alternating interactions. Four typical systems with interactions of FPU-$\beta$ and Toda types, respectively, are mainly considered here. To produce each temperature profile, the Nose-Hoover heat baths [27] with temperatures $T_+ = 3.0$ and $T_- = 2.0$ are coupled to two left- and rightmost particles, and the velocity-Verlet algorithm [28]

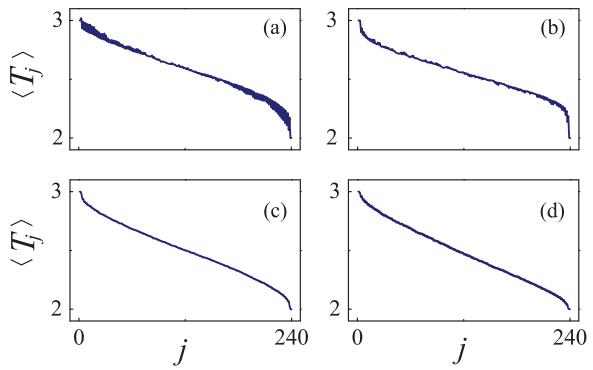


FIG. 2. (Color online) The temperature profile for the diatomic lattice [(a) and (b)] and the lattice with alternating interactions [(c) and (d)] with system size $L = 240$. For each lattice the mass (coupling) ratio $r$ is 0.25. In (a) and (c) the interparticle interactions take the FPU-$\beta$ type; in (b) and (d) they take the Toda type.

with a time step 0.005 is used to evolve the system. After the system is evolved for a long enough time, we then examine the temperature distribution along the lattice. The results for a fixed mass (coupling) ratio $r = 0.25$ are summarized in Fig. 2, from which a more well-behaved temperature profile for the lattices with alternating interactions than the diatomic lattices, regardless of the interaction types, can be clearly seen. It is worth mentioning that such an advantage has also been verified for other mass (coupling) ratios, suggesting that the thermalization problem has been successfully avoided.

Then we examine the normal modes for both lattices, aiming at tracing the origin of the thermalization problem. Such a consideration is based on the understanding from Ref. [21] that it is the dependence of the mean kinetic energy of a particle on normal modes inducing the thermalization problem. With this in mind we shall particularly focus on modes in the $q \to 0$ and $q \to \pi/2$ limits, since they represent the limiting behaviors of particles' vibrations. We consider the diatomic lattice first. Supposing $x_{2j-1} = Ae^{[i\omega_q t - iq(2j-1)]}$ and $x_{2j} = Be^{[i\omega_q t - iq(2j)]}$ as the normal mode solutions, then, under the first condition $q \to 0$ we have $A/B = 1$ for acoustic modes and $A/B = -1$ for optical modes, where $B$ ($A$) represents the vibration amplitude of the particle $2j$ ($2j - 1$) [1]. This result means that for $q = 0$ the adjacent particles vibrate in phase for acoustic modes but out of phase for optical modes. Thus, the reason for their name as acoustic mode and optical mode is clear. Under the second condition $q \to \pi/2$, we get $A/B = 0$ ($B/A = 0$) for acoustic (optical) modes. Such a result means that for $q = \pi/2$, only one of the adjacent particles can move for both kinds of modes. Now according to the understanding [21], the reason for the thermalization problem in the diatomic lattices can be understandable: the modes that only one of the adjacent particles moves are generally existing in these systems, which may lead to a large difference of the mean kinetic energy between the adjacent particles, and thus results in the ill-behaved temperature profile.

Now let us turn to the lattice with alternating interactions. Under the first condition $q \to 0$ and according to Eq. (4) we have $\omega_q^- = 0$ and $\omega_q^+ = \sqrt{2(k_1 + k_2)}$. Substituting them into Eq. (2) or (3) we get $A/B = 1$ ($A/B = -1$) for acoustic (optical) modes, which is similar to that in diatomic lattices. While for the second condition $q \to \pi/2$ the situation is quite different. Following the same analysis we have $A/B = -i$ ($A/B = i$) for acoustic (optical) modes. This result means that for $q = \pi/2$ the adjacent particles vibrate with a phase difference of $\pm\pi/2$, in contrast to the fact that only one of the adjacent particles moves in diatomic lattices. Then based on the understanding from Ref. [21], a large difference of the mean kinetic energy between the adjacent particles may not occur, thus, the thermalization problem is avoided.

Combining the above analysis, now the reason for proposing the lattice model with alternating interactions here is obvious: it not only has a linear phonon spectra with tunable phonons similar to that in diatomic lattice but also is free of the thermalization problem. Thus, in the following we shall make use of this lattice to study the heat conduction properties for FPU-$\beta$ system, exploring the role the optical phonons may play in heat transport.

## III. HEAT CONDUCTION

We employ the reverse nonequilibrium molecular dynamics (RNEMD) method to study the heat conduction properties of this system. This approach has been first proposed by Müller-Plathe [29] for monoatomic fluids and then extended by Bedrov *et al.* [30] to be applicable to molecular fluids with internal constraints. The vasp [31,32] and lammps [33] code modified to the RNEMD method is reported later. For the method applying to 1D lattice systems, we have recently presented a detailed implementation [19].

To adopt the RNEMD method, the heat flux is imposed by dividing the lattice into sections of equal size and exchanging kinetic energy (velocity swapping here) between the hot and cold sections. This exchange then in turn results in the temperature gradient. Compared with the usual method that directly brings the two ends of the lattice in contact with two heat baths at different temperatures to impose the heat flux, the RNEMD method has its advantages: it can suppress the boundary effects by applying the periodic boundary conditions, and thus leads to a faster convergence to the stationary state. This advantage has been well verified in our previous work [19].

We start the simulations with a fully thermalized lattice at a temperature $T = 2.5$. For compatibility with this temperature, we take the exchange frequency to be 0.1 in adopting the RNEMD method. We employ the velocity-Verlet algorithm [28] with a time step of 0.005 to evolve the system. After the nonequilibrium stationary state has been established, we then examine the temperature profiles. As an example, Fig. 3(a) shows the typical temperature profile with system size $L = 4992$ for $r = 0.25$, from which a well-behaved temperature profile can be clearly seen. Obviously, the thermalization problem is absent here. We note that such a well-behaved temperature has also been verified for other $r$ values. Based on this fact, we are able to measure the heat flux and finally obtain the heat conductivity according to Fourier's law. To measure the heat flux, usually a transient stage of time no less than $10^6$, which has been verified to be long enough for reaching the stationary state, is discarded; then the next evolution of time $10^7$ is performed for the time average. We have also verified

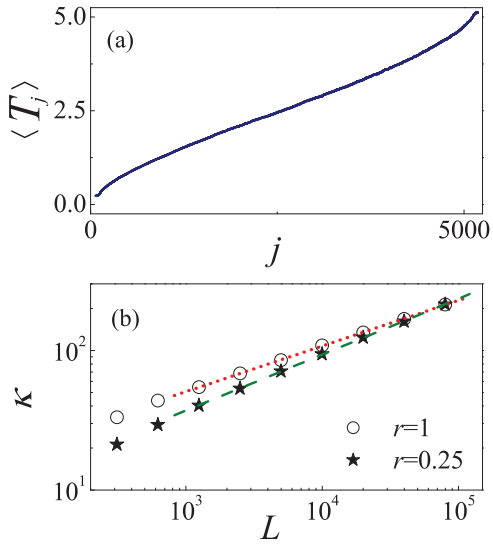


FIG. 3. (Color online) (a) The temperature profile for the lattice with alternating interactions for coupling ratio $r = 0.25$ and system size $L = 4992$. Here the RNEMD method is used to produce such a profile; (b) the heat conductivity $\kappa$ versus $L$ for $r = 1$ and $r = 0.25$, where the dashed (dotted) line is for the best fitting of $\kappa \sim L^{\alpha}$, suggesting that $\alpha = 0.325 \pm 0.002$ for $r = 1$ (dotted) (see also Ref. [19]) and $\alpha = 0.408 \pm 0.002$ for $r = 0.25$ (dashed), respectively. Note that in (b) the error bars (not shown) are smaller than the symbol size.

that our results do not significantly depend on the particular simulation details taken here.

Having derived the heat conductivity $\kappa$, we are then able to examine the size dependence of $\kappa$. The result for $r = 0.25$ is shown in Fig. 3(b), from which $\kappa \sim L^{\alpha}$ can be clearly recognized; it suggests $\alpha = 0.408 \pm 0.002$. This result is in agreement with the power-law divergent behavior of heat conductivity in 1D momentum conserving lattices with symmetric interactions [14,15]. For comparison, the dependence of $\alpha$ on $L$ for $r = 1$, the monatomic FPU-$\beta$ lattice, is also plotted in Fig. 3(b); it suggests $\alpha = 0.325 \pm 0.002$ (see Ref. [19]). Combing both results, we find that although the value of $\kappa$ for $r = 0.25$ is smaller than that for $r = 1$ at a small $L$, it will finally overtake due to having a larger $\alpha$. The size to see such a reversing is around $L \sim 10^4$–$10^5$. Since the main difference between $r = 1$ and $r = 0.25$ is whether the optical phonons are introduced, a larger $\alpha$ implies that optical phonons can enhance heat transport in the thermodynamical limit, i.e., $L \to \infty$. The small size effects of $\kappa$ may mainly be induced by the simultaneous reduction of the group velocity of acoustic phonons when the optical phonons are introduced [see Fig. 1(b)].

Do other $r$ values lead to the above picture? To answer this question we carefully examine the results of $\alpha(r)$, which are summarized in Fig. 4. Therein two data points are extracted from Fig. 3(b) while others are calculated additionally in the same way. From Fig. 4 one can see that as $r$ decreases from 1 to 0, $\alpha$ increases first, reaches its maximum value $\alpha_{\max} \approx 0.4$ at $r_{\rm tr} = 0.25$, then decreases down to $\alpha \approx 1/3$ for $r \to 0$. Thus, compared with $r = 1$, $\alpha$ can be generally enhanced for $r \neq 1$, but this enhancement is nonmonotonic; it will disappear for $r \to 0$. The result for $r \to 0$ is reasonable because $r = 0$ suggests $k_1 \ll k_2$, which indicates that one can

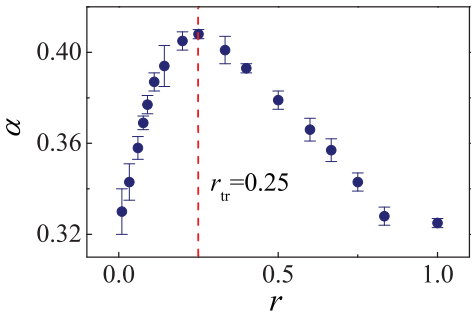


FIG. 4. (Color online) The dependence of $\alpha$ on the coupling ratio $r$. The vertical dashed line indicates $r_{\rm tr} = 0.25$. Error bars give the standard error for evaluating $\alpha$ by linearly fitting $\ln \kappa$ versus $\ln L$.

treat the adjacent particles with coupling $k_2$ as a whole, hence the system with $r \to 0$ is equivalent to a monatomic FPU-$\beta$ lattice with coupling $k_1$ only, then $\alpha \approx 1/3$. Interestingly, in the intermediate range of $r$, $\alpha$ changes continuously and nonmonatomically with a turning point at $r_{\rm tr} = 0.25$, which is in clear contrast to the argument [12] that even the optical phonons are introduced, $\alpha$ is the same as that in 1D monatomic FPU-$\beta$ lattices without optical phonons.

## IV. DISCRETE BREATHERS

Now we understand that optical phonons can also enhance heat transport. In this section we discuss its mechanism. From our current knowledge on the mechanism of heat transport properties in monatomic FPU-$\beta$ lattices [19], we shall relate it to the properties of discrete breathers (DBs) [34]. DBs have been shown to have great contribution to heat conduction, i.e., the properties of $\alpha$, in 1D rotator lattices [35] and 1D FPU-$\beta$ lattices with both nearest-neighbor coupling and next-nearest-neighbor coupling [19]. Nevertheless, these studies are concerned with the monatomic lattices whose linear phonon spectra containing only acoustic modes. When the diatomic lattices or the lattices with alternating interactions where the linear phonon spectra contains both acoustic modes and optical modes are taken into account, the situation may be quite different. The DBs properties studied in diatomic lattices [36–46] indeed support this difference, i.e., a new kind of DBs, the gap DBs with frequencies lying in the gap between acoustic modes and optical modes can emerge when the mass ratio is appropriate [46]. However, in spite of these studies, at present whether and, if yes, what roles the gap DBs would play in heat transport is still an open question. Motivated by this, we are particularly interested in the DBs properties of our systems and try to relate it with the results observed in Sec. III.

To study the DBs properties, we should obtain DBs at the focused temperature $T = 2.5$ first. We employ the following method [47]: A lattice of 1000 particles is initially thermalized to $T = 2.5$ with Nose-Hoover heat baths [27]; then the heat baths are removed, and the absorbing boundary conditions are imposed [48]. If DBs exist, after a long enough time for absorption, leading all the mobile excitations, such as phonons and solitary waves absent, they may show up in the internal segment of the lattice. In this way DBs can be identified. As some examples, the snapshots of the energy profile of the residual thermal fluctuations for several $r$ are plotted in Fig. 5,

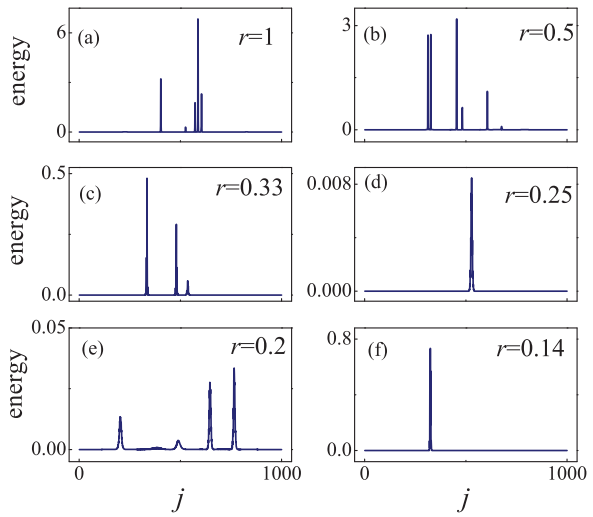


FIG. 5. (Color online) Snapshots of the energy distribution of the residual thermal fluctuations for $r = 1$ (a); $r = 0.5$ (b); $r = 0.33$ (c); $r = 0.25$ (d); $r = 0.2$ (e); $r = 0.14$ (f), respectively.

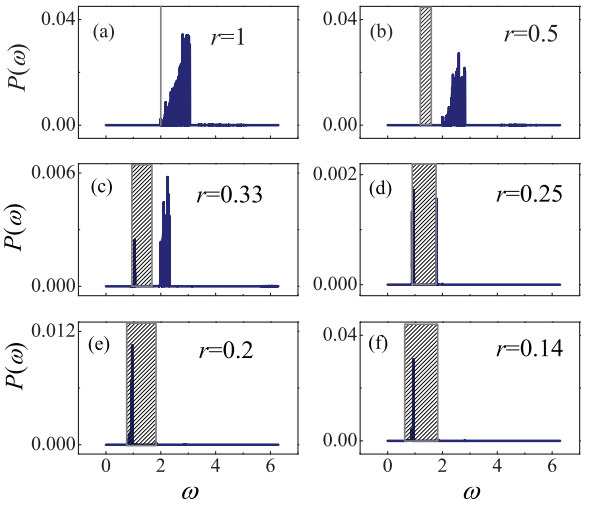


FIG. 6. (Color online) The power spectrum of the residual thermal fluctuations for $r = 1$ (a); $r = 0.5$ (b); $r = 0.33$ (c); $r = 0.25$ (d); $r = 0.2$ (e); $r = 0.14$ (f), respectively, all of which take arbitrary units. The shaded area indicates the gap of the linear spectra between the acoustic branch and the optical branch for each $r$ [see Fig. 1(b)]. Notice that for $r = 1$ the gap is absent.

from which a well-recognized snapshot of DBs for each $r$ can be clearly seen. We have verified that this is also the case for other $r$ values lying in $[0,1]$, suggesting that DBs can indeed exist in our systems. Some other details that should be mentioned are that the linewidth of the DBs energy profiles for different $r$ is different, especially for $r$ values below and above $r_{\rm tr} = 0.25$, indicating that the properties of DBs for different $r$ may be quite different. Thus, it may be desirable to discuss the space shapes of these DBs, which will be presented in our further studies [49].

In order to identify the gap DBs, next we calculate the power spectra $P(\omega)$ of the residual thermal fluctuaions [see Fig. 5]. We recall that $P(\omega)$ for $\omega > 2$ corresponds to the optical DBs [36,37] and $P(\omega)$ for $\omega$ in the gap between the acoustic and optical branches corresponds to the gap DBs [40] first.

To measure $P(\omega)$, for each $r$, we take 100 instances of simulation where different initial conditions are used, for the average. For each instance, initially we start with a short lattice of $N = 200$ particles (for facilitating the computation) that was fully thermalized to the focused temperature by using Nose-Hoover heat baths [27], then the heat baths are removed and the absorbing boundary conditions are imposed [19]. After the absorbing has been implemented for a long enough time, we will obtain the DBs (shown in Fig. 5) and then calculate the $P(\omega)$ for all particles along the lattice, which just gives the spectra of all DBs.

In Fig. 6, the results of $P(\omega)$ for the $r$ values investigated in Fig. 5 are plotted. The shaded area in each panel of Fig. 6 indicates the gap between the optical and the acoustic branches of the linear phonon spectrum [see Fig. 1(b)]. As $r$ decreases from 1 to 0, we may find that for larger $r$ values [see Figs. 6(a) and 6(b)], $P(\omega)$ has nonzero value only for $\omega > 2$, suggesting that all DBs are optical DBs. As $r$ decreases, a new nonzero part of $P(\omega)$ whose frequency components fall in the spectrum gap and slightly above the acoustic branch, will appear [see Fig. 6(c)], suggesting the emergence of one family of gap DBs. More interestingly, if $r$ is decreased further, in a narrow range of $0.2 < r < 0.33$, a second family of gap DBs arises, whose frequency components are slightly below the optical branch instead [see Fig. 6(d)]. It is worth noting that $r = 0.25$ is a turning point, at which the two kinds of gap DBs have close spectrum strength. Finally, for smaller $r$ values ($0 < r < 0.2$), the second family of gap DBs would disappear and only the first family would survive. Therefore, our system is featured by three families of DBs, one for optical DBs and two for the gap DBs, characterized by their frequencies, respectively. As the system parameter $r$ changes from 1 to 0, a transition from the optical DBs to the gap DBs takes place. Such a feature is similar to that as observed in the diatomic FPU-$\beta$ lattices [38,39], which is interesting and whose details will be discussed elsewhere [49].

Another detail in Fig. 6 that should be mentioned is that all the DBs lie outside the linear phonon band, suggesting that they all belong to the extraband DBs. We note that DBs can be mainly classified into two categories, i.e., the intraband DBs (with frequencies within the linear phonon band) and the extraband DBs. We also emphasize that the roles of intraband DBs and extraband DBs play in heat transport are quite different, i.e., the extraband DBs may mainly localize energy, but the intraband DBs can be scattering with phonons since they have frequencies within the linear phonon band. In some systems the intraband DBs can also be observed. For example, we have shown a possible picture for the role the intraband DBs play in heat conduction in Ref. [19].

Now let us turn to explaining the heat transport properties observed in Fig. 4. As only the extraband DBs exist in our system, we define $\eta = \int_0^\infty P(\omega)d\omega / \int_0^\infty P_0(\omega)d\omega$, the ratio of the residual energy after the absorption to the initial energy, to measure the localization of energy induced by DBs, where $P_0(\omega)$ and $P(\omega)$ are the power spectra of the initial thermal fluctuations and that after the absorption, respectively. Then it is expected that a smaller $\eta$ leads to less energy localization and will finally facilitate heat transport in the thermodynamical

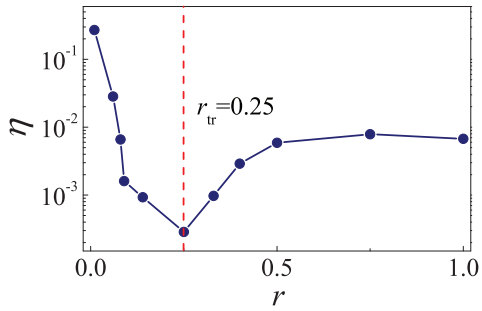


FIG. 7. (Color online) The energy portion $\eta$ of the residual thermal fluctuations after a long enough time for absorption versus $r$.

limit. For several additional $r$ values, we have calculated the corresponding power spectrum in the same way as in Fig. 6 and evaluated $\eta$, finally summarized in the results in Fig. 7, from which one can see that as $r$ decreases from 1 to 0, $\eta$ decreases first, reaches its minimum value at $r_{tr} = 0.25$, then increases. Because a smaller $\eta$ indicates a larger $\alpha$ for heat conduction, the explanation from Fig. 7 is in accord with the results of Fig. 4.

## V. CONCLUSIONS

To summarize, in order to study the effects of optical phonons on heat conduction, we have studied the 1D lattice model with alternating interactions. Compared with the diatomic lattices, our model is advantageous because it avoids the thermalization problem. Our main finding is that introducing the optical phonons can enhance heat transport in the thermodynamical limit. This finding suggests that the effects of optical phonons on heat transport cannot be neglected simply because they have relatively small group velocities compared with acoustic phonons. In addition, our study has related the enhancement of heat conduction to the properties of DBs. We find that two kinds of extraband DBs, the optical DBs and the gap DBs, can generally exist in our model system, and a change from the optical DBs to the gap DBs with the coupling ratio can take place. During this change, the DBs release energy and thereby enhance the heat transport.

Finally, we would like to point out that to enhance heat transport in our system, only introducing the optical phonons is inadequate, the anharmonic (nonlinear) interactions may also play an essential role. A possible picture is that the anharmonicity causes a resonance between acoustic and optical phonons, such as the second-harmonic generation found in diatomic lattices [50], and if this resonance is appropriate, the heat transport would be enhanced. The DBs shown in Figs. 5 and 6 just act as the bridge of this resonance. The gap (described by coupling ratio $r$) between the acoustic and optical phonons branches can then be regarded (or assumed) as the length of bridge, which we emphasize that is also of great importance. Our result suggests that $r$ should be neither too long, nor too short, and maybe $r_{tr} = 0.25$ is the best.

So the results in Figs. 5–7 just present some primary evidences to support the picture of the mechanism on the interactions between optical phonons and heat transport. To establish a more complete picture, further detailed investigations are still required.

## ACKNOWLEDGMENTS

We thank J. Wang for carefully reading the manuscript and providing valuable discussions. We also thank A. Dhar for his useful comments. This work is supported by the NNSF of China (Grants No. 11205032, No. 10925525, No. 11147191, and No. 10805036), the NSF of Fujian province (Grant No. 2013J05008) and the start-up fund of Fuzhou University (Grant No. 022390).

[1] C. Kittel, *Introduction to Solid State Physics* (Wiley, New York, 1996).
[2] Y. Chen, D. Li, J. R. Lukes, and A. Majumdar, J. Heat Transfer **127**, 1129 (2005); D. L. Nika, E. P. Pokatilov, A. S. Askerov, and A. A. Balandin, Phys. Rev. B **79**, 155413 (2009); E. Muñnoz, J. Lu, and B. I. Yakobson, Nano Lett. **10**, 1652 (2010).
[3] L. Yang, N. Yang, and B. Li, Sci. Rep. **3**, 1143 (2013).
[4] P. G. Klemens, Phys. Rev. **148**, 845 (1966).
[5] C. Hess and B. Bchner, Eur. Phys. J. B **38**, 37 (2004).
[6] I. Terasaki, H. Tanaka, A. Satake, S. Okada, and T. Fujii, Phys. Rev. B **70**, 214106 (2004).
[7] M. Kazan, S. Pereira, J. Coutinho, M. R. Correia, and P. Masri, Appl. Phys. Lett. **92**, 211903 (2008).
[8] A. Mittal and S. Mazumder, J. Heat Transfer **132**, 052402 (2010).
[9] J. Shiomi and S. Maruyama, Phys. Rev. B **73**, 205420 (2006); S. Jpn. J. Appl. Phys. **47**, 2005 (2008).
[10] Z. Tian, J. Garg, K. Esfarjani, T. Shiga, J. Shiomi, and G. Chen, Phys. Rev. B **85**, 184303 (2012).
[11] C. Jeong and M. Lundstrom, Appl. Phys. Lett. **100**, 233109 (2012).
[12] A. Dhar and K. Saito, Phys. Rev. E **78**, 061136 (2008).
[13] T. Mai, A. Dhar, and O. Narayan, Phys. Rev. Lett. **98**, 184301 (2007).
[14] S. Lepri, R. Livi, and A. Politi, Phys. Rep. **377**, 1 (2003).
[15] A. Dhar, Adv. Phys. **57**, 457 (2008).
[16] O. Narayan and S. Ramaswamy, Phys. Rev. Lett. **89**, 200601 (2002).
[17] A. Pereverzev, Phys. Rev. E **68**, 056124 (2003); J.-S. Wang and B. Li, Phys. Rev. Lett. **92**, 074302 (2004); Phys. Rev. E **70**, 021204 (2004); L. Delfini, S. Lepri, R. Livi, and A. Politi, *ibid.* **73**, 060201(R) (2006); J. Stat. Mech. (2007) P02007; G. R. Lee-Dadswell, B. G. Nickel, and C. G. Gray, J. Stat. Phys. **132**, 1 (2008).
[18] H. vanBeijeren, Phys. Rev. Lett. **108**, 180601 (2012).
[19] D. Xiong, J. Wang, Y. Zhang, and H. Zhao, Phys. Rev. E **85**, 020102(R) (2012).
[20] Y. Zhong, Y. Zhang, J. Wang, and H. Zhao, Phys. Rev. E **85**, 060102(R) (2012); S. Chen, Y. Zhang, J. Wang, and H. Zhao, arXiv:1204.5933; arXiv:1208.0888.

[21] V. Kannan, A. Dhar, and J. L. Lebowitz, Phys. Rev. E **85**, 041118 (2012).
[22] J. J. Xiao, K. Yakubo, and K. W. Yu, Phys. Rev. B **73**, 054201(R) (2006).
[23] L. Kavitha, A. Muniyappan, A. Prabhu, S. Zdravković, S. Jayanthi, and D. Gopi, J. Biol. Phys. **39**, 15 (2013); A. Shimizu *et al*., J. Am. Chem. Soc. **132**, 14421 (2010).
[24] J. H. Luscombe, Phys. Rev. B **36**, 501 (1987).
[25] L. L. Concalves and J. P. de Lina, J. Phys.: Condens. Matter **9**, 3447 (1997).
[26] M. Alaghemandi, J. Schulte, F. Leroy, F. Müller-Plathe, and M. C. Bohm, J. Comput. Chem. **32**, 121 (2011).
[27] S. Nose, J. Chem. Phys. **81**, 511 (1984); W. G. Hoover, Phys. Rev. A **31**, 1695 (1985).
[28] M. P. Allen and D. L. Tildesley, *Computer Simulation of Liquids* (Clarendon, Oxford, 1987).
[29] F. Müller-Plathe, J. Chem. Phys. **106**, 6082 (1997).
[30] D. Bedrov and G. D. Smith, J. Chem. Phys. **113**, 8080 (2000).
[31] S. Stackhouse, L. Stixrude, and B. B. Karki, Phys. Rev. Lett. **104**, 208501 (2010).
[32] D. Wang, L. Tang, M. Long, and Z. Shuai, J. Phys. Chem. C **115**, 5940 (2011).
[33] http://lammps.sandia.gov
[34] S. Flach and C. R. Willis, Phys. Rep. **295**, 181 (1998); S. Aubry, Physica D **216**, 1 (2006); S. Flach and A. V. Gorbach, Phys. Rep. **467**, 1 (2008).
[35] O. V. Gendelman and A. V. Savin, Phys. Rev. Lett. **84**, 2381 (2000); C. Giardina, R. Livi, A. Politi, and M. Vassalli, *ibid*. **84**, 2144 (2000).
[36] V. M. Burlakov, S. A. Kiselev, and V. N. Pyrkov, Solid State Commun. **74**, 327 (1990); M. Aoki, J. Phys. Soc. Jpn. **61**, 3024 (1992).
[37] R. Livi, M. Spicci, and R. S. MacKay, Nonlinearity **10**, 1421 (1997).
[38] G. James and P. Noble, Physica D **196**, 124 (2004).
[39] T. Cretegny, R. Livi, and M. Spicci, Physica D **119**, 88 (1998); G. James and M. Katner, Nonlinearity **20**, 631 (2007).
[40] M. E. Manley, D. L. Abernathy, N. I. Agladze, and A. J. Sievers, Sci. Rep. **1**, 4 (2011).
[41] M. E. Manley, A. J. Sievers, J. W. Lynn, S. A. Kiselev, N. I. Agladze, Y. Chen, A. Llobet, and A. Alatas, Phys. Rev. B **79**, 134304 (2009).
[42] M. E. Manley, Acta Mater. **58**, 2926 (2010).
[43] L. Z. Khadeeva and S. V. Dmitriev, Phys. Rev. B **84**, 144304 (2011).
[44] S. V. Dmitriev, A. A. Sukhorukov, A. I. Pshenichnyuk, L. Z. Khadeeva, A. M. Iskandarov, and Yu. S. Kivshar, Phys. Rev. B **80**, 094302 (2009)
[45] Y. Doi, A. Nakatani, and K. Yoshimura, Phys. Rev. E **79**, 026603 (2009).
[46] L. Z. Khadeeva and S. V. Dmitriev, Phys. Rev. B **81**, 214306 (2010).
[47] G. P. Tsironis, A. R. Bishop, A. V. Savin, and A. V. Zolotaryuk, Phys. Rev. E **60**, 6610 (1999).
[48] G. P. Tsironis and S. Aubry, Phys. Rev. Lett. **77**, 5225 (1996).
[49] D. Xiong, Y. Zhang, J. Wang, and H. Zhao (unpublished).
[50] V. V. Konotop, Phys. Rev. E **54**, 4266 (1996).